Jianxin Tang
Seth Fraden
Martin Fisher School of Physics
Brandeis University
Waltham, MA 02254

Nonmonotonic Temperature Dependence of the Flexibility of Bacteriophage *fd*

We present two experiments that probe the temperature dependence of the flexibility of the filamentous virus fd *by examining aspects of the liquid crystalline nature of* fd *suspensions. The first measurement is of the temperature variation of the coexisting* fd *concentrations at the isotropic–cholesteric phase transition. The second measurement is of the magnetic field induced birefringence or Cotton–Mouton constant in the isotropic phase as a function of temperature. We compare these measurements with the theoretical treatment of Onsager, Khokhlov–Semenov, and Chen and conclude that the flexibility of* fd *varies nonmonotonically with temperature and has a minimum in persistence length at 35°C.* © *1996 John Wiley & Sons, Inc.*

INTRODUCTION

In this paper we present measurements of the temperature-dependent persistence length of the bacteriophage *fd*, a long, thin, semiflexible, and charged virus. Rather basic statistical mechanical theories predict that a colloidal suspension of semiflexible rodlike charged particles undergo a first-order phase transition between an orientationally isotropic (I) and an orientationally ordered, nematic or cholesteric liquid crystalline phase (A).[1,2] The transition is entropically driven, and for neutral polymers the volume fractions of the two coexisting phases depend solely on the contour length to diameter ratio and the persistence length to contour length ratio. Since *fd* is charged, the I–Ch transition also depends on ionic strength and varies from 0.5 to 2% volume fraction as the ionic strength increases from 1 to 100 mM.[3] Quantitative agreement between the theory of the I–Ch transition at a single temperature and experiment was observed,[3] establishing *fd* as a model colloidal liquid crystal.[4] Review articles summarizing research in virus-based liquid crystals tobacco mosaic virus (TMV)[5] and *fd*[4] have recently appeared.

The theoretical model of the liquid crystalline phase behavior considered in this paper applies equally well to either the nematic or cholesteric phase. In each phase particles have short-range or liquid-like correlations between the centers-of-mass, but long-range correlations between the angle of alignment of the long axes of the particles. The distinction between the two ordered phases is that particles in the nematic phase prefer to be parallel to each other, while in the cholesteric phase the alignment direction precesses in a helical fashion.[6] The *fd* suspensions form a cholesteric phase (Ch) and the I–Ch transition at a single temperature has been investigated extensively.[3,4,7–9] In this paper, we report measurements of the temperature dependence of *fd* coexistence concentrations and find a maximum in the concentrations at 35°C. Adopting the premise that *fd* suspensions are well described by theory,[1–4,10] we suggest that a nonmonotonic temperature-dependent variation of the flexibility of *fd* accounts for the variation in the concentrations of the coexisting phases.

The specific magnetic field induced birefringence (Δn) in the isotropic phase provides information on two interesting quantities. In the limit

Received May 22, 1995; accepted September 22, 1995.
Biopolymers, Vol. 39, 13–22 (1996)

CCC 0006-3525/96/010013-10

of low *fd* concentration and low magnetic field (H), $\Delta n/H^2$ is proportional to concentration and is a function of the polymer flexibility,[11] as well as the anisotropy of the particle's optical and magnetic susceptibilities. At higher concentrations (but low fields), pretransitional angular correlations between the particles cause $\Delta n/H^2$ to nonlinearly increase with concentration and eventually diverge at ρ^*, the spinodal concentration of the isotropic phase.[3,9,12] This concentration dependence of Δn permits determination of ρ^*,[2-4] which also depends on the flexibility of the particle. The birefringence study in this report is focused on relating the temperature-dependent flexibility to the measured Δn and ρ^* values, and correlating these measurements with the phase coexistence data.

MATERIAL AND PROPERTIES

The *fd* is a virus of 880 nm contour length (L), diameter 6.6 nm (D),[13] and persistence length (P) of 2.2 μm measured at $T = 22°C$.[14-18] The *fd* is negatively charged at pH 7.3,[19] with an approximate charge density of 10 e/nm and has a molecular weight 1.64×10^7 g/mol.[13,20] We attempted to characterize polydispersity with electromicroscopy, electrophoresis,[21] and analytical centrifugation. A large distribution in lengths was observed in negative-stained transmission electron micrograph photographs, but we suspect the drying process causes both fracturing and aggregation of the virus. Very narrow distributions were observed in both electrophoresis and analytical centrifugation, but no attempt to quantify the length distribution was made. An additional indirect assay of the length distribution is that we have observed a smectic liquid crystalline phase in samples of 3–10% volume fraction as a function of ionic strength.[4,7,22] Since slight polydispersity suppresses the smectic phase, we conclude that the viruses are highly monodisperse. While the structure of *fd* is known to high resolution,[13,23] in this paper we model *fd* virus as a smooth, uniformly charged, semiflexible rod.

COEXISTENCE CONCENTRATIONS

Theory

Onsager developed a statistical mechanical theory of the isotropic to nematic phase transition of a suspension of charged rigid rods.[1] He noted that an expansion of the free energy in the powers of concentration provides a theory of the phase transition whose accuracy increases with the ratio of the length to diameter of the particles. Khokhlov and Semenov[2,24,25] generalized Onsager's approach to include systems of semiflexible chains in the limit that both $L \gg D$ and $P \gg D$, but with arbitrary value of L/P. Khokhlov and Semenov solved their model analytically in the limit of $L \gg P$, and Chen [10] has reported an accurate numerical calculation of the Khokhlov–Semenov model for arbitrary flexibility (L/P).

The numerical results of the isotropic (c_i) and cholesteric (c_c) coexistence concentrations as a function of flexibility are[10]

$$c_i = \frac{4.1895 + 26.1020\alpha + 66.0026\alpha^2 + 117.846\alpha^3}{1 + 3.4806\alpha + 9.0331\alpha^2} \tag{1}$$

$$\omega = \frac{0.2737 + 3.0357\alpha + 3.0666\alpha^2 + 10.7859\alpha^3}{1 + 26.8263\alpha + 86.7892\alpha^2 + 143.145\alpha^3} \tag{2}$$

with $c_x = L^2 D n_x$ the dimensionless concentration, x being either the isotropic (i) or cholesteric (c) phase, n_x the number density, $\alpha = L/P$ the flexibility parameter, and $\omega = (c_c - c_i)/c_i$ the fractional difference between the coexisting phases.

Onsager demonstrated that the dominant effect of charge can be accounted for by introducing a charge-dependent effective diameter D_{eff}, which is larger than the hard rod diameter D. D_{eff} is calculated by finding the separation of the rods at which the energy of repulsion equals kT as averaged over the angular distribution function $f(\Omega)$ in the isotropic phase.[1] For *fd* in an 1:1 electrolyte, D_{eff} can be readily calculated as a function of ionic strength.[3,26] In order to compare with experimental measurements, we convert the dimensionless number concentrations c_x to mass concentrations in mg/mL, ρ_x:

$$\rho_x = m \frac{c_x}{L^2 D_{\text{eff}}} \tag{3}$$

where m is the mass of an individual particle. The predicted coexistence concentrations ρ_x as a function of D_{eff} are in good agreement with experiment.[3,4]

It should be noted here that there is a smaller additional factor in determining the coexistence concentrations, which scales as $\kappa^{-1}/D_{\text{eff}}$, the ratio of the Debye screening length to the effective diam-

eter. Correction of the theoretical coexistence concentrations due to this effect is predicted to be on the order of 10%,[26-28] but it is ignored in our treatment for co-existence concentrations.

Temperature Dependence of the Coexistence Concentrations of *fd*

In contrast to TMV, where the isotropic–nematic coexistence concentrations were temperature independent,[29] we report here that for *fd* the isotropic–cholesteric coexistence concentrations varied in a nonmonotonic fashion with temperature over the range 4–70°C. We studied a *fd* virus solution of approximately 20 mg/mL that was dialyzed against 10 m*M* potassium phosphate (KP) buffer solution at pH 7.3. Phosphate was chosen because of the weak temperature dependence of the pH. However, a disadvantage of phosphate is that it is polyvalent, which complicates the calculation of the interparticle potential.[26] The sample after dialysis was carefully diluted to the coexistence region and sealed with a rubber cover in a small clean glass tube of roughly 40 mm in length and 6 mm in diameter. Then the tube was immersed, but kept vertical, in a temperature-controlled water tank and allowed sufficient time to phase separate. The phase separation in the bulk was slow due to the small difference in the specific gravity between the two coexisting phases, and also the viscosity was large due to the length of the virus particles. Frequently, a table centrifuge was used to apply up to 1000 g to speed the separation after the isotropic and cholesteric phases separated into micron-sized droplets after standing at 1 g overnight. The temperature at which the sample was equilibrated was not always maintained during centrifugation, so the samples were spun in successive intervals of a few minutes each and the sample tube was replaced in the temperature bath immediately following each centrifugation. The equilibration time for the samples to phase separate was days and was much longer than the few minutes that the sample was in the nontemperature-controlled centrifuge.

After thorough phase separation into an isotropic phase in the upper portion of the tube and a cholesteric in the bottom portion, a sample of volume 20 μL or so was carefully pipetted from each phase while observing through crossed polarizers. The samples were immediately weighed with an analytical balance of 0.01 mg accuracy and subsequently diluted approximately 50-fold to measure the *fd* mass concentration by optical spectrophotometry. It was necessary to thoroughly mix the two-phase samples after changing the temperature because otherwise it would take an extremely long time for the individual coexisting isotropic and cholesteric phases to change concentration purely by diffusion. In other words, care must be taken to avoid metastable states, while mixing the samples allows them to reach equilibrium. Repeated measurements showed that the variation of the coexistence concentrations between different samples prepared under what was intended to be identical conditions occasionally reached 5%.

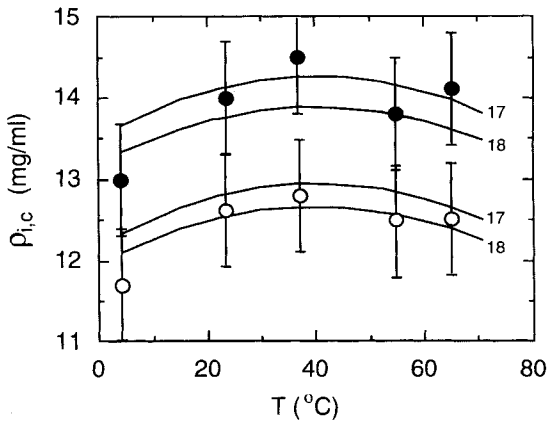

FIGURE 1 Coexistence concentrations of isotropic ρ_i (○) and cholesteric ρ_c (●), measured at five temperatures. A maximum in coexistence concentrations is observed near 35°C. Error bars indicate 5% variation for each concentration. The labeled solid lines correspond to the theoretical predictions of ρ_i and ρ_c for $D_{\text{eff}} = 17$ and 18 nm where the temperature dependence of the flexibility of *fd* was extracted from Figure 2. Coexistence concentrations for intermediate values of D_{eff} lie parallel to the solid lines and fall within the textured regions.

In Figure 1, the I–Ch coexistence concentrations of *fd* are shown at five temperatures. A 5% error bar was assigned to each data point, for which three independent measurements were done. However, since we always measured ρ_i and ρ_c in the same sample, the relative difference between the coexistence concentrations $\omega = (\rho_c - \rho_i)/\rho_i$ was reliably measured to be about $\omega \sim 10\%$ at each temperature. The remarkable feature of the temperature dependence of the coexistence concentrations is that a maximum was observed at about 35°C. The temperature-induced shift in coexistence concentrations is not large, amounting to about a 5% variation between the highest and lowest concentrations.

In a previous paper[3] we established that the Khokhlov–Semenov (KS) theory quantitatively described the coexistence concentrations of the iso-

tropic–cholesteric phase (I–Ch) of *fd* suspensions. Here, we take the view that the temperature dependence of the I–Ch concentrations arises solely from the variation of the flexibility of *fd* with temperature. We assume that the KS theory is accurate and use the measured I–Ch concentrations to extract the flexibility α. In order to compare the measured ρ_i and ρ_c at room temperature (23°C) with the theoretical prediction from Eqs. (1)–(3), we use $L = 880$ nm and $m = 1.64 \times 10^7$ g/mol. In principle, D_{eff} can be numerically calculated by solving the nonlinear Poisson–Boltzmann equation with full consideration of the polyvalent ion composition of the KP buffer. However, this was not carried out in our study and calculations of D_{eff} were done assuming a monovalent solution.[3] The ionic strength of 10 mM KP at pH 7.3 is 24 mM, while the ion concentration of K^+ is 17 mM, which is the major counterion for the negatively charged *fd* particles in solution. The "extra" ionic strength comes from the negative divalent phosphate ions. The variation in D_{eff} is not great for this range of ionic strengths and assuming a linear charge density of 1 e/Å [19] we find $D_{\text{eff}} = 18$, 17, and 16 nm for ionic strengths 17, 20, and 24 mM, respectively. Here, comparisons with theory were done assuming D_{eff} in the range of 17–18 nm.

The solid smooth curves drawn in Figure 1 for the temperature dependence of the I–Ch phase boundary were obtained through a different method, which is explained in the following subsection.

ρ_i and ρ_c Through Percentage Determination

An alternative method for determining coexistence concentrations as functions of temperature is to measure the percentage of the cholesteric portion of the sample in coexistence, instead of directly measuring the concentrations as before. Approximately 100 μL of *fd* sample in coexistence was permanently sealed by oxygen flame in a glass capillary about 8 cm in length, which was then treated the same way in the water bath as the glass tubes described earlier. Since the capillaries have uniform cross section, the percentage of cholesteric is easily determined by measuring the ratio of height of the cholesteric to the total sample with a ruler. More importantly, since the fractional difference in concentration between the coexistence phases ω is small, and always about 10%, the percentage shift of the amount of cholesteric phase is approximately 10 times the percentage change of the concentration of either phase. This magnifying effect arises from the conservation of the total virus in a sealed capillary, which can be written as

$$\rho_i(1-f) + \rho_c f = \rho_i(1+f\omega) = \rho_{\text{ave}} \qquad (4)$$

with f the fraction of the cholesteric, ρ_i the concentration of the isotropic, and ρ_{ave} the average concentration of the total solution. For example, if following a temperature change the isotropic concentration changes as $\rho_i \rightarrow 0.95\rho_i$, and the width of the coexistence region ω remains 0.1, then f increases by about 50% according to Eq. (4). Thus a 5% change in the coexistence concentrations is translated into a 50% shift in the height of the coexistence phase boundary.

There is a serious drawback to this method due to the observation of a slight irreversible change of the *fd* samples with time. At room temperature, the coexistence concentrations shift higher with time, and such a shift persisted for months during our experiment with the sample sealed in capillaries. As previously, we thoroughly mix the two phase suspension upon each change in temperature. A day or two is usually necessary to reach complete separation of the new equilibrium phases following every temperature change, even with the help of gentle centrifugation. A typical cycle consisting of one measurement following every 5°C temperature change through the temperature range 4–70°C takes 3–4 weeks, during which period the coexistence concentrations shift upward about 1%. This very slight change is easily measured as a change in the height of the I–Ch meniscus. The rate of shift is dependent on temperature and is larger at high temperatures. At 4°C, the sample stays stable for months. This shift rate also depends on the ionic strength, and we observed more rapid changes at the lower ionic strengths. The physical origin of such a shift is not well understood. We note that both electron microscopy and electrophoresis experiments detected no significant difference between a fresh stock of *fd* and a well-sealed *fd* solution that had suffered through months of temperature cycles.

Figure 2 shows the percentage of cholesteric phase in one sample capillary of $\rho_{\text{ave}} = 13.0 \pm 0.3$ mg/mL, 10 mM phosphate buffer, pH 7.3, as a function of temperature. The temperature was sequentially cycled from low to high values (circles), and then from high to low (triangles). Since the total material in each tube is constant, an increase in the coexistence concentrations results in a decrease of the percentage of the cholesteric phase.

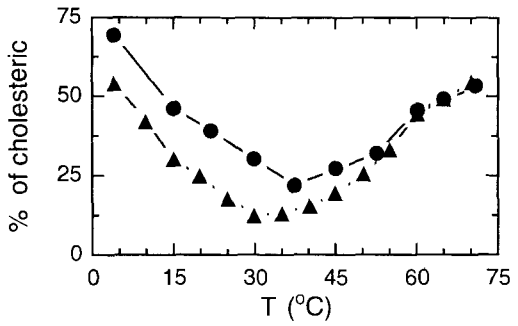

FIGURE 2 Percentage of the cholesteric in coexistence with the isotropic phase as a function of temperature, measured in a sealed capillary of the total liquid length 82.2 mm. The temperature was cycled once from low to high temperature (circles), and then back from high to low once (triangles). The total experiment was completed in about two months, over which time the percentage of the cholesteric at 4°C decreased about 15%. The decrease in the percentage of the cholesteric phase from 4 to 35°C corresponds to an increase in the coexistence concentrations of about 5%, a result consistent with the data of Figure 1.

From the beginning to the end of the measurements shown in Figure 2, a period of two months, the percentage of the cholesteric phase decreased from 70 to 55%, which amounts to only a 1.5% shift in the coexistence concentrations. While a direct measurement of a 5% shift in coexistence concentrations shown in Figure 1 is close to the limit of experimental accuracy, here such a shift corresponds to a height change of the isotropic–cholesteric meniscus of 4 cm, an easily measured effect.

Our previous measurements of the coexistence concentrations of *fd* as a function of ionic strength[3] were in excellent agreement with Chen's[10] numerical results of the Khokhlov and Semenov theory.[2,25] If we accept this theory as being applicable to the *fd* system, then we conclude that the temperature dependence of the I–Ch transition arises from the temperature dependence of the flexibility of *fd*. Chen[10] provides explicit formulae [Eqs. (1)–(2)] for the dependence of concentration of the coexisting isotropic phase c_i and the width of the coexistence concentrations ω. In turn, c_i is proportional to ρ_i through Eq. (3). These equations are functions of two quantities we treat as unknowns: (1) the ratio of contour to persistence length of the particle, and (2) the effective diameter D_{eff}. We first fix D_{eff} to be either 17 or 18 nm, as discussed above, and then fit the percentage of cholesteric data f shown in Figure 2 as solid symbols to Eq. (4) in order to extract the persistence length. The results of the fit of the persistence length are shown in Figure 3.

The persistence length P has been independently measured by light scattering to be $P = 2.2$ μm at 20°C.[15–18] Inspection of Figure 3 reveals that this persistence length corresponds to an effective diameter $D_{\text{eff}} \approx 17.8$ nm for the persistence length obtained from the coexistence measurements. We find that the persistence length decreases about 15–30% over the temperature range 4–35°C and then increases again by nearly the same amount from 35 to 70°C. It would be interesting if independent confirmation of the temperature dependence of the flexibility could be made by another technique, such as light scattering.

The determination of the temperature dependence of the persistence length allows us to predict the isotropic–anisotropic coexistence concentrations using Eqs. (1)–(3). These predictions are drawn in Figure 1 as solid lines.

MAGNETIC-FIELD-INDUCED BIREFRINGENCE

Cotton–Mouton Effect

The *fd* has a positive anisotropy of the diamagnetic susceptibility $\Delta\chi$, which means that the rods tend

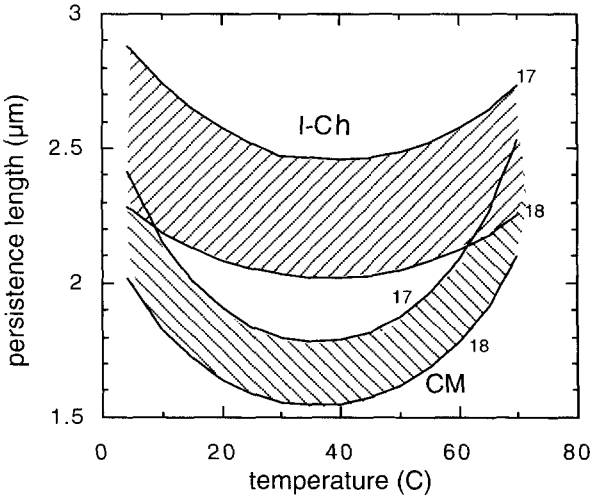

FIGURE 3 The upper set of curves labeled "I–Ch" are the persistence length P of *fd* as a function of temperature deduced from the measurements of the percentage of the cholesteric phase in coexistence with the isotropic shown in Figure 2. The numbers 17 and 18 indicate the values of D_{eff} in nm used in the fit of the data of Figure 2 to the Eqs. (3) and (4). The lower set, labeled "CM," are deduced from magnetic birefringence measurements of ρ^* shown in Figure 6 and fitted to Eq. (7). The temperature dependence for intermediate values of D_{eff} lie parallel to the limiting values of D_{eff}.

to align parallel to an applied magnetic field H.[30] The particles are also optically anisotropic and when partially aligned by the field the entire suspension becomes birefringent. In the limit of weak magnetic field, the field-induced birefringence Δn is proportional to the square of the magnetic field. It is instructive to consider the specific birefringence $\Delta n/\rho$, with ρ the particle mass density, as the response per particle to an external stimulus H^2. The ratio of this response to stimulus is then the susceptibility of a particle in suspension to align parallel to the field. The specific magnetic susceptibility or specific Cotton–Mouton (CM) constant is defined to be

$$\mathrm{CM} \equiv \frac{\Delta n}{\rho H^2} \tag{5}$$

We have recently derived the following expression for a suspension of persistent polymers,[3]

$$\mathrm{CM} = \mathrm{CM}|_{\rho\to 0}\left(1 - \frac{\rho}{\rho^*}\right)^{-1} \tag{6}$$

where

$$\rho^* = m\frac{16}{\pi D_{\mathrm{eff}} L^2}\frac{g(\alpha)}{(1 - 3h/4)} \tag{7}$$

and[30]

$$\mathrm{CM}|_{\rho\to 0} = \frac{\Delta N_{\mathrm{sat}}\Delta\chi}{15kT\lambda}\frac{1}{g(\alpha)} \tag{8}$$

with $\Delta\chi$ the anisotropy of the magnetic susceptibility for a fully straightened persistent polymer, and ΔN_{sat} the maximum birefringence per unit concentration in full alignment, $\Delta N_{\mathrm{sat}} = \Delta n_{\mathrm{sat}}/\rho$. Charged rods of the same sign held at a fixed separation have the lowest energy when they are crossed. This tendency of charged rods to twist is manifested in Eq. (7) by the parameter h known as the twisting constant $h = \kappa^{-1}/D_{\mathrm{eff}}$, where κ^{-1} the Debye screening length.[26] In our case where we assume an effective ionic strength of 17–18 mM we calculate $h = 0.13$.[3] Equations (7) and (8) contain a common term:

$$g(\alpha) = \left\{\frac{1}{3\alpha}\left[1 - \frac{1}{3\alpha}(1 - e^{-3\alpha})\right]\right\}^{-1} \tag{9}$$

where α is the flexibility parameter defined in the section on the theory of coexistence concentrations. For a rigid rod $\alpha = 0$ and $g(0) = 1$, while for a worm-like chain $\alpha \gg 1$ and $g(\alpha) \sim 3\alpha/2$.

One can provide the following interpretation for Eq. (6): In the absence of a field, the particles in the isotropic phase point in all directions with equal probability when averaged over the entire sample and the suspension is optically isotropic. However, locally there are angular correlations between neighboring rods, and the correlation length increases with concentration. Application of a magnetic field aligns these correlated regions along the field, and the field-induced birefringence is proportional to the number of particles in a correlation volume N_{corr}.[29,30] It follows that N_{corr} is given by the ratio of the susceptibility at finite concentration to the susceptibility in the limit of zero concentration or

$$N_{\mathrm{corr}} = \frac{\mathrm{CM}}{\mathrm{CM}|_{c\to 0}} = \frac{1}{1 - \rho/\rho^*} \tag{10}$$

All of the concentration dependence of the Cotton–Mouton constant of Eq. (6) is contained in N_{corr}.

In Eq. (6), ρ^* is the concentration at which the Cotton–Mouton constant and N_{corr} becomes infinite—hence ρ^* is the limiting concentration above which an isotropic phase becomes absolutely unstable, i.e., the spinodal concentration of the isotropic branch of the phase diagram.[24,31] However, at a concentration less than ρ^* the suspension becomes nematic via a first-order phase transition, which in the Onsager model occurs when $N_{\mathrm{corr}} = 5.7$.[32] From Eq. (7) we see that if the twisting constant h exceeds the value $\frac{4}{3}$, then ρ^* is infinite, which means the nematic phase has been destabilized by charge.[24,26] In the case of *fd*, h is 10 times less then this critical value. In our previous study of the isotropic–cholesteric phase transition,[3] we concluded that the most significant effect of charge is to alter the effective diameter with the destabilization of the twisting term being a minor perturbation to the phase transition.

Experiment

Magnetic-field-induced optical birefringence measurements were performed with a 20 T Bitter magnet at the Francis Bitter National Magnet Laboratory. We used a photoelastic modulation and 2-lock-in amplification setup.[4,33] The measured field-induced phase shift[34] is related to the birefringence Δn and the orientational order parameter S as follows

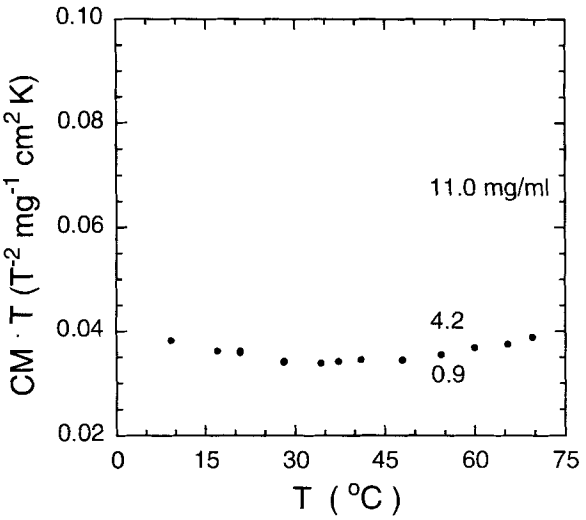

FIGURE 4 CM · T, the product of the specific Cotton–Mouton constant and the absolute temperature, which is proportional to the number of particles in a correlation volume N_{corr}, is plotted as a function of temperature (T) for three concentrations. At constant temperature, N_{corr} grows with increasing concentration. Each data set at constant concentration was measured following increases of temperature from 8.5 to 70°C plus a repeat of the 20°C measurement to check that the CM constant was reversible. Each curve shows a well-defined minimum at about 35°C.

$$S = \frac{\Delta n}{\Delta n_{sat}} = \frac{\lambda \Delta \phi}{2\pi d \Delta n_{sat}} \qquad (11)$$

where $\lambda = 633$ nm, $d = 3.0$ mm is the sample path length, and Δn_{sat} is the birefringence of the *fd* sample in full alignment.

We have measured the field-induced birefringence Δn of *fd* as a function of temperature for several concentrations of *fd* in the isotropic phase. At low values of the field, Δn is proportional to the square of the magnetic field (H^2), and the Cotton–Mouton constant CM [Eq. (5)] was determined by fitting a straight line to the measured Δn vs H^2. However, for concentrated samples near the isotropic–cholesteric phase transition, we observed a large nonlinear increase in Δn with H^2 and eventually at the highest fields a saturation behavior occurred. This and further studies of a field-induced isotropic–nematic phase transition have been described elsewhere.[35]

Figure 4 is a plot of CM · T, the product of the specific Cotton–Mouton constant and the absolute temperature, as a function of temperature T. The point of this plot is to remove the explicit temperature dependence from Eq. (8). Data from three different *fd* concentrations are shown in the graph. The increase of the CM constant with concentration at constant temperature results from the increase in the angular correlation number N_{corr}. The study of the concentration dependence of N_{corr} has been reported elsewhere.[3] Here we draw attention to the following features: (1) Each data point was obtained from a sequential series measurements beginning from 8.5 to 70°C, and ending by repeating a measurement at 20°C. The CM constant was reproduced within 2% between the two measurements at 20°C, suggesting no irreversible change in the sample through measurements up to 70°C. (2) All three curves show a well-defined minimum at about 35°C, which is consistent with observations of the temperature variation of the coexistence concentrations discussed previously. It is therefore suggestive to assume that the temperature variations of both the coexistence concentrations and the magnetic susceptibility are governed by the temperature variation of the flexibility of *fd*. (3) Note that the relative change of the CM data with temperature increases with concentration. We observed in Figure 1 that the coexistence concentrations are a maximum at 35°C. This means that ρ^*, the concentration where the CM constant diverges, is also a maximum at 35°C. Lowering ρ^* at fixed concentration ρ by either increasing or decreasing the temperature from 35°C causes N_{corr} and thus the CM constant to increase. Furthermore, the percentage change in CM with temperature will increase as the concentration ρ approaches ρ^*. At low concentrations $N_{corr} \sim 1$ and varies little with temperature. The remaining observed temperature dependence in CM · T at low concentrations comes from temperature variations in single particle properties such as $\Delta\chi$ and the persistence length of the virus as expressed in Eq. (8).

Equation (6) states that the inverse of the specific Cotton–Mouton constant, 1/CM, decreases linearly with concentration ρ. This should hold at any fixed temperature, and has been observed for *fd*[3] and TMV.[29,36] In Figure 5(a), we show 1/CM as a function of concentration at the three temperatures of 8.5 (○), 40 (●), and 70°C (△). A few of the measurements were not done at precisely these three specified temperatures, in which case a simple linear interpolation between adjacent temperatures in Figure 4 was performed. This treatment does not introduce much error, since the measured birefringence changes smoothly and by a small amount for a temperature variation of a few degrees. The solid lines in Figure 5 are the linear fits of the data to Eq. (6) for the different labeled tem-

peratures, and extrapolations to $1/CM = 0$ determine ρ^*, while extrapolations to $\rho = 0$ determine $1/CM|_{\rho \to 0}$. Note the nonmonotonic temperature behavior of ρ^*. Figure 5(b) displays the same plots as in Figure 5(a) with a slight modification to the vertical axis, for which $1/(CM \cdot T)$ is plotted instead of $1/CM$. This removes the explicit dependence of temperature from Eq. (8). The remaining temperature dependence can only arise from a combination of the variation of the flexibility factor $g(\alpha)$ and $\Delta N_{sat}\Delta\chi$ in Eq. (8). Note in Figure (5b) the solid lines of linear fits are roughly parallel.

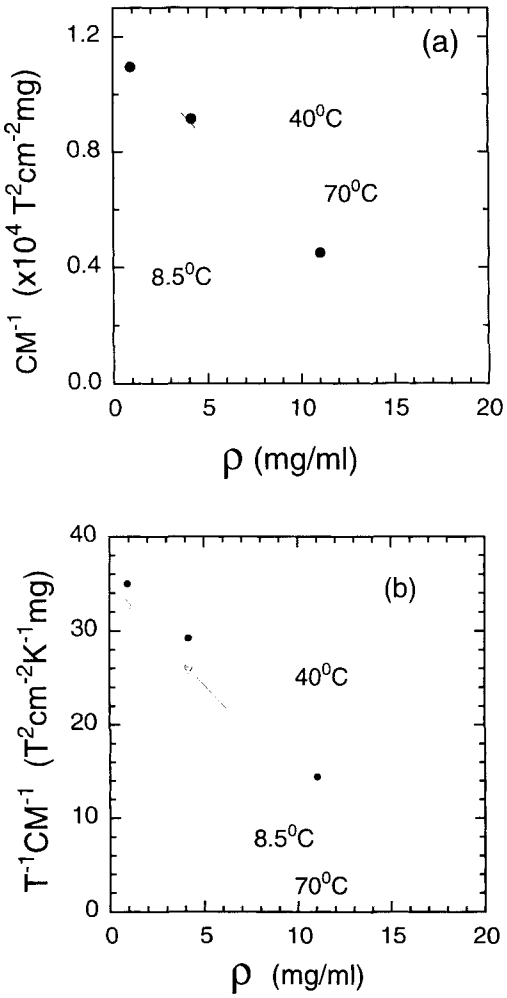

FIGURE 5 (a) The inverse of the specific Cotton–Mouton constant CM^{-1} as a function of the concentration ρ. Data were chosen from Figure 4 at three temperatures: 8.5°C (○), 40°C (●), and 70°C (△). Each solid line is a linear fit to Eq. (6) from which ρ^* and $CM|_{\rho \to 0}$ were determined. (b) $CM \cdot T$ as function of ρ. The linear fits are roughly parallel for the three temperatures, which from Eqs. (6)–(8) implies that the product $\Delta N_{sat}\Delta\chi$ is independent of temperature.

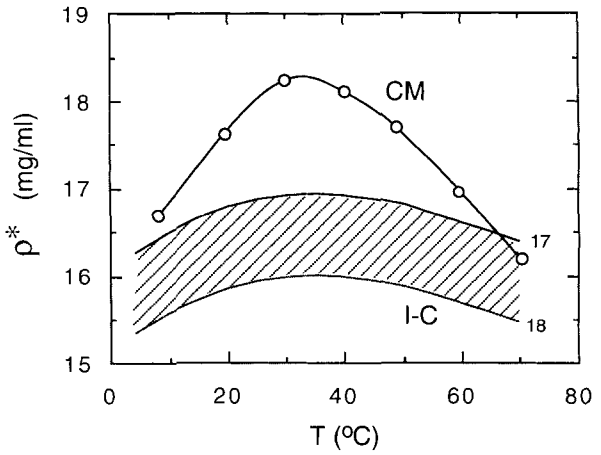

FIGURE 6 The limit of stability or spinodal concentration of the isotropic phase ρ^* as a function of temperature measured in two different ways. Data with hollow circles are obtained from the CM measurements illustrated in Figure 5, while the lower continuous curves are obtained using Eq. (7) with $g(\alpha)$ extracted from the temperature dependence of the I–C coexistence concentrations shown in Figures 1 and 2, and with $D_{eff} = 17$ and 18 nm.

According to Eqs. (6)–(8), the slope of the lines in Figure (5b) is $(T \cdot CM|_{\rho \to 0} \cdot \rho^*)^{-1}$ and will be independent of temperature only if $\Delta N_{sat}\Delta\chi$ is independent of temperature.

In Figure 6, we show ρ^* as determined by the CM measurements and also by the measurements of the coexistence concentrations. The ρ^* from the CM measurements are shown as hollow circles at seven temperatures, and were obtained through the extrapolations partially shown in Figure 5(a) or (b). This measurement of ρ^* is purely experimental. On the other hand, the continuous solid curves at the bottom are ρ^* calculated from Eq. (7) using the temperature-dependent persistence length extracted from the isotropic–cholesteric coexistence concentrations shown in Figure 3 for two values of D_{eff}. These two different methods of determining ρ^* give the same answer within 10%, and furthermore show the same temperature dependence with a maximum in ρ^* at 35°C.

Conversely, having experimentally obtained ρ^* from the CM data, we can use Eq. (7) to extract $g(\alpha)$ and hence the persistence length. The persistence length determined this way is shown in Figure (3), along with the persistence length obtained from the measurement of the coexistence concentrations, shown in Figures 1 and 2. These two methods of determining the persistence length agree within 25%, and both show the same nonmonotonic

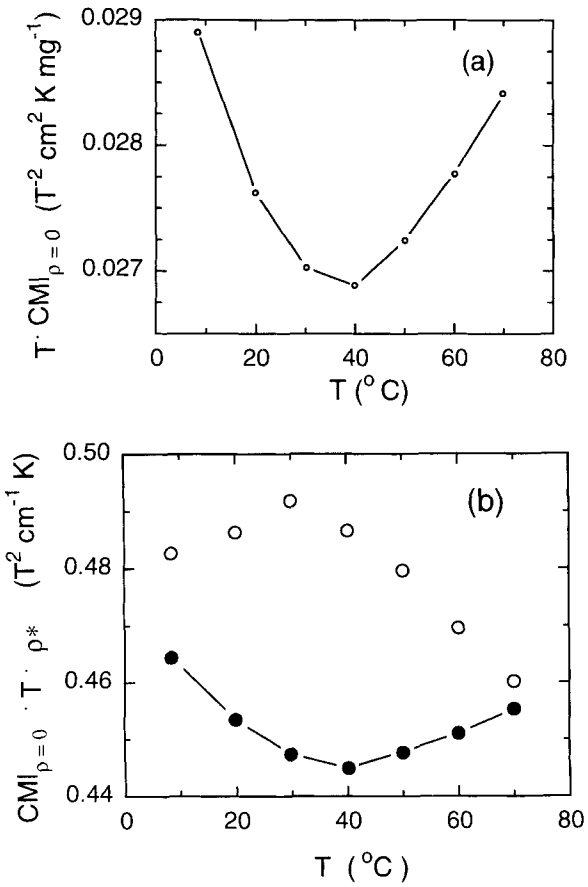

FIGURE 7 (a) The product of temperature and the Cotton–Mouton constant in the limit of infinite dilution $T \cdot CM|_{\rho \to 0}$ is plotted as a function of temperature. This product is proportional to $\Delta N_{sat} \Delta\chi / g(\alpha)$. (b) The product $CM|_{\rho \to 0} \cdot T \cdot \rho^*$ is proportional to $\Delta N_{sat} \Delta\chi$. The values of ρ^* were obtained through the magnetic birefringence measurements (○) or from the coexistence concentration measurements (●) as shown in Figure 6 with $D_{eff} = 17.4$ nm.

temperature variation of the flexibility of *fd* with a minimum in persistence length at 35°C.

In Figure 7(a) we plot $T \cdot CM|_{\rho \to 0}$ vs temperature, using data obtained from Figures 4 and 5. From Eq. (8) we expect this quantity to be proportional to $\Delta N_{sat} \Delta\chi / g(\alpha)$. In principle, any of these terms could account for the observed temperature dependence. However, we can isolate the temperature dependence of the product $\Delta N_{sat} \Delta\chi$ by examining the product $CM|_{\rho \to 0} \cdot T \cdot \rho^*$, which according to Eqs. (7) and (8) will be proportional to $\Delta N_{sat} \Delta\chi$. In Figure 7(b) we show $CM|_{\rho \to 0} \cdot T \cdot \rho^*$ obtained with the two measurements of ρ^* that were illustrated in Figure 6. As seen in Figure 7(b) the two sets of values of $CM|_{\rho \to 0} \cdot T \cdot \rho^*$ vs T have opposite curvature. As a consequence, we are unable to draw any conclusions about the temperature dependence of $\Delta N_{sat} \Delta\chi$ other than this product varies less than 5%.

CONCLUSIONS

We have observed the temperature dependence of the isotropic–cholesteric coexistence concentrations of filamentous bacteriophage *fd* in colloidal suspension. The coexistence concentrations vary nonmonotonically with temperature and have maximum values at about 35°C. The variation of the coexistence concentrations of approximately 5% in the temperature range of 4–70°C was directly determined by measuring the optical absorbance upon dilution, and more precisely by measuring the percentage variation of coexistence phases with fixed average concentration.

Measurements of the magnetic-field-induced birefringence of *fd* as a function of concentration and temperature allowed determination of the limit of stability of the isotropic phase ρ^*. The nonmonotonic temperature variation of ρ^* was similar to that of the coexistence concentrations.

We analyzed the direct measurements of the coexistence concentrations and the measurement of ρ^* from the magnetic birefringence experiments in terms of the Onsager–Khokhlov–Semenov theory of the isotropic–nematic phase transition. This permitted two determinations of the temperature dependence of the persistence length of *fd*. The two determinations gave somewhat different answers, but both consistently described the persistence length as having a minimum length of approximately 2 μm at 35°C and increasing by 10–30% as the temperature was varied ±35°C.

Through monitoring the coexistence concentrations and by measuring the magnetic-field-induced birefringence as a function of temperature, we have probed the change of *fd* flexibility with great sensitivity, and are able to detect variations in the persistence length as small as 10–20%. The methods used can be applied to the study of other semiflexible polymers in solution, including biopolymers such as DNA and actin.

REFERENCES

1. Onsager, L. (1949) *Ann. NY Acad. Sci.* **51,** 627.
2. Khokhlov, A. R. & Semenov, A. N. (1982) *Physica* **112A,** 605.

3. Tang, J. & Fraden, S. (1995) *Liquid Crystals.* **19,** 459.
4. Fraden, S. (1995) in *Observation, Prediction, and Simulation of Phase Transitions in Complex Fluids,* Nato-ASI, Course CXXIX, Baus, M., Rull, L. F. & Ryckaert, J. P., Eds., Kluwer Academic Publishers, pp. 113–164.
5. Meyer, R. B. (1990) in *Dynamics and Patterns in Complex Fluids,* Springer Proceedings in Physics, Vol. 52, Onuki, A. & Kawasaki, K., Eds., Springer-Verlag, New York, p. 62.
6. deGennes, P. G. & Prost, J. (1993) *The Physics of Liquid Crystals,* 2nd ed., Oxford Science, New York.
7. Lapointe, J. & Marvin, D. A. (1973) *Mol. Cryst. Liquid Cryst.* **19,** 269.
8. Oldenbourg, R. (1981) Ph.D. thesis, Universität Konstanz, Germany.
9. Nakamura, H. & Okano, K. (1983) *Phys. Rev. Lett.* **50,** 186.
10. Chen, Z. Y. (1993) *Macromolecules* **26,** 3419.
11. Maret, G. & Weill, G. (1983) *Biopolymers* **22,** 2727.
12. Photinos, P., Rosenblatt, C., Schuster, T. M. & Saupe, A. (1987) *J. Chem. Phys.* **87,** 6740.
13. Day, L. A., Marzec, C. J., Reisberg, S. A. & Casadevall, A. (1988) *Ann. Rev. Biophys. Chem.* **17,** 509.
14. Beck, K. & Duenki, R. M. (1990) *J. Struct. Biol.* **105,** 22.
15. Loh, E., Ralston, E. & Schumaker, V. N. (1979) *Biopolymers* **18,** 2549.
16. Loh, E. (1979) *Biopolymers* **18,** 2569.
17. Maeda, T. & Fujime, S. (1985) *Macromolecules* **18,** 2430.
18. Song, L., Kim, U.-S., Wilcoxon, J. & Schurr, J. M. (1991) *Biopolymers* **31,** 547.
19. Zimmermann, K., Hagedorn, J., Heuck, C. C., Hinrichsen, M. & Ludwig, J. (1986) *J. Biol. Chem.* **261,** 1653.
20. Newman, J., Swinney, H. L. & Day, L. A. (1977) *J. Mol. Biol.* **116,** 593.
21. Griess, G. A., Moreno, E. T., Herrmann, R. & Serwer, P. (1990) *Biopolymers* **29,** 1277.
22. Booy, F. P. & Fowler, A. G. (1985) *Int. J. Biol. Macromol.* **7,** 327–335.
23. Glucksman, M. J., Bhattacharjee, S. & Makowski, L. (1992) *J. Mol. Biol.* **226,** 455–470.
24. Odijk, Th. (1986) *Macromolecules* **19,** 2313.
25. Semenov, A. N. & Khokhlov, A. R. (1986) *Sov. Phys. Usp.* **31,** 988–1014.
26. Stroobants, A., Lekkerkerker, H. N. W. & Odijk, Th. (1986) *Macromolecules* **19,** 2232.
27. Vroege, G. J. (1989) *J. Chem. Phys.* **90,** 4560.
28. Chi, S.-M. & Chen, Z. Y. (1994) *Macromolecules* **27,** 6124.
29. Fraden, S., Maret, G. & Caspar, D. L. D. (1993) *Phys. Rev. E* **48,** 2816.
30. Maret, G. & Dransfeld, K. (1985) in *Strong and Ultrastrong Magnetic Fields and Their Applications,* Herlach, F., Ed., Springer-Verlag, New York.
31. Kayser, R. F., Jr. & Ravechè, H. J. (1978) *Phys. Rev. A* **17,** 2067.
32. Straley, J. P. (1973) *Mol. Cryst. Liquid Cryst.* **22,** 333.
33. Fuller, G. G. (1990) *Ann. Rev. Fluid Mech.* **22,** 387.
34. Torbet, J. & Maret, G. (1981) *Biopolymers* **20,** 2657.
35. Tang, J. & Fraden, S. (1993) *Phys. Rev. Lett.* **71,** 3509.
36. Fraden, S., Maret, G., Caspar, D. L. D. & Meyer, R. B. (1989) *Phys. Rev. Lett.* **63,** 2068.